Bosonization of the interacting Su-Schrieffer-Heeger model

Jin, Zizhuo Tony; Ruggiero, Paola; Giamarchi, Thierry

How to cite

JIN, Zizhuo Tony, RUGGIERO, Paola, GIAMARCHI, Thierry. Bosonization of the interacting Su-Schrieffer-Heeger model. In: Physical Review B, 2023, vol. 107, n° 20, p. L201111. doi: 10.1103/PhysRevB.107.L201111

This publication URL: https://archive-ouverte.unige.ch/unige:174333

Publication DOI: 10.1103/PhysRevB.107.L201111

Letter

Bosonization of the interacting Su-Schrieffer-Heeger model

Tony Jin,[1,2,*] Paola Ruggiero,[3] and Thierry Giamarchi[1]
[1]*DQMP, University of Geneva, Quai Ernest-Ansermet 24, CH-1211 Geneva, Switzerland*
[2]*Pritzker School of Molecular Engineering, University of Chicago, Chicago, Illinois 60637, USA*
[3]*King's College London, Strand, London WC2R 2LS, United Kingdom*

(Received 2 January 2023; accepted 10 May 2023; published 17 May 2023)

We derive the bosonization of the interacting fermionic Su-Schrieffer-Heeger (SSH) model with open boundaries. We use the classical Euler-Lagrange equations of motion of the bosonized theory to compute the density profile of the zero-energy edge mode and observe excellent agreement with numerical results, notably the localization of the mode near the boundaries. Remarkably, we find that repulsive or attractive interactions do not systematically localize or delocalize the edge mode but their effects depend on the value of the staggering parameter. We provide quantitative predictions of these effects on the localization length of the edge mode. Our study shows that bosonization is able to quantitatively describe edge modes of interacting topological one-dimensional systems and pave the way to generalization to other models.

DOI: 10.1103/PhysRevB.107.L201111

Topological concepts have become a central part of contemporary condensed matter physics [1]. The understanding of the geometrical and topological objects underpinning band theory [2–5] has fostered intense activities in diverse areas of condensed matter physics such as the study of the quantum Hall effect [6,7], spin-orbit induced topological band insulators [8–10], topological quantum computing [11], and so on and so forth.

One current limitation of topological band theory is its restriction to noninteracting systems. Interactions will in general spoil the band structure, rendering usual classification schemes inoperative. There, novel phenomena may be expected, the most famous example being the fractional quantum Hall effect [12].

One of the simplest models capturing the key features of topological insulators is the Su-Shrieffer-Heeger (SSH) model [13]. The fermionic SSH model consists of a one-dimensional (1D) tight-binding model with alternating bond value. Depending on whether the first bond is weak or strong, the model is either in the topological or trivial phase. For open boundaries, one possible characterization of the topological phase is the presence of twofold, quasidegenerate, zero-energy edge modes that are exponentially localized at the boundaries. Remarkably, these edge modes have been observed and characterized experimentally in one-dimensional optical lattices [14] and artificial spin chains simulated with Rydberg atoms [15] in ultracold atoms setup.

To treat interactions in 1D systems, a powerful technique that was developed in the previous decades is *bosonization* [16,17].

One trademark ability of bosonization is to map interacting spinless fermions in 1D to a *free* bosonic theory. Remarkably, this technique has been successfully applied to study the effects of interactions on Majorana modes in superconducting wires [18–22]. However, to the best of our knowledge, despite extensive analytical and numerical studies of the bulk physics and phase diagram of the interacting SSH (see, e.g., Refs. [23–27]), it has yet to be determined whether bosonization is able to describe quantitatively the physics of the edge modes.

In this Letter, we fill this gap by deriving the bosonized theory of the interacting SSH model with open boundaries. We use the classical Euler-Lagrange (EL) equations of motion of the bosonized theory to compute the density profile of the zero-energy edge mode and observe excellent agreement with numerical results, notably the localization of the mode near the boundaries. Remarkably, we find that repulsive or attractive interactions do not systematically localize or delocalize the edge mode but their effects depend on the value of the staggering parameter. We provide quantitative predictions of these effects on the localization length. Our results are a proof of concept that bosonization is able to describe the edge modes of interacting topological 1D systems and pave the way to a generalization to other models.

We begin by discussing the bosonization procedure in the absence of interactions. Let $(c_j, c_j^\dagger)_{j\in[1,N]}$ be the usual fermionic creation and annihilation operators associated to site j. The discrete free SSH Hamiltonian on N sites in 1D is given by

$$H = \sum_{j=1}^{N-1} [-t - \delta(-1)^j](c_j^\dagger c_{j+1} + \text{H.c.}), \tag{1}$$

i.e., we have a tight-binding chain with alternating values for the bond. Fixing $t > 0$, the topological phase corresponds to the case where we have an *even* number of sites and $\delta > 0$. A signature of the topological phase is the existence for open boundary conditions of quasidegenerate zero-energy eigenstates [28] in which a single particle is in a coherent superposition between the two edges of the chain—

*tonyjin@uchicago.edu.ch

see, e.g., Refs. [29,30] for details on the noninteracting case.

The fermionic operator c_j for open boundaries can be expanded in Fourier modes $\tilde{c}_n$ as

$$c_j = i\sqrt{\frac{2}{N+1}}\sum_{n=1}^{N}\tilde{c}_n \sin\left(\frac{\pi jn}{N+1}\right). \tag{2}$$

For $\delta = 0$, this rotation diagonalizes the problem, i.e., we have $H_{\delta=0} = \sum_n \varepsilon_n \tilde{c}_n^\dagger \tilde{c}_n$ with $\varepsilon_n \equiv -2t\cos(\frac{\pi n}{N+1})$.

The continuum limit is obtained by introducing the lattice spacing a and defining the position $x \equiv ja$ and the momentum $k \equiv \frac{2\pi n}{2a(N+1)}$. The size of the system is taken to be $L \equiv a(N+1)$ so that $k = \frac{\pi n}{L}$. The continuous fermionic field is $\Psi(x) \equiv \frac{1}{\sqrt{a}}c_j$. The boundary conditions for Ψ are obtained by extending the discrete formula Eq. (2) to site 0 and site $N+1$: $\Psi(x=0) = 0$ and $\Psi(x = a(N+1) = L) = 0$.

Following the usual bosonization procedure [17,31], we split Ψ into left- and right-moving fields $\Psi_{\mathrm{L/R}}$ by expanding around the Fermi energy ε_{k_F}:

$$\Psi(x) = \Psi_{\mathrm{R}}(x) + \Psi_{\mathrm{L}}(x), \tag{3}$$

$$\Psi_{\mathrm{R}}(x) = \sqrt{\frac{L}{2}}e^{ik_F x}\int_{-\infty}^{\infty}\frac{dk}{\pi}\tilde{c}_{k+k_F}e^{ikx}, \tag{4}$$

$$\Psi_{\mathrm{L}}(x) = -\Psi_{\mathrm{R}}(-x). \tag{5}$$

For convenience, we also define the "slow" fields $\mathrm{R}(x) \equiv \Psi_{\mathrm{R}}(x)e^{-ik_F x}$, $\mathrm{L}(x) \equiv e^{ik_F x}\Psi_{\mathrm{L}}(x)$. Importantly, because of open boundaries, the left and right movers are *not* independent as is encapsulated by Eq. (2)—see, e.g., Refs. [32–34] for previous discussions of open boundary bosonization.

In the continuum, $\mathrm{R}(x)$ taken alone can be thought of as a field living on a space of size $2L$ with *periodic boundary conditions*. In the bosonized language, it can then be reexpressed as

$$\mathrm{R}(x) = F_{\mathrm{R}}\frac{1}{\sqrt{2\pi\alpha}}e^{i\phi_R(x)}, \tag{6}$$

$$\phi_{\mathrm{R}}(x) \equiv \frac{\pi x}{L}N_{\mathrm{R}} + \sum_{n>0}\frac{1}{\sqrt{n}}\left(a_n e^{i\frac{n\pi x}{L}} + a_n^\dagger e^{-i\frac{n\pi x}{L}}\right)e^{-\alpha\frac{\pi n}{2L}}, \tag{7}$$

where F_{R} is the Klein factor [17] associated to the right mover with $F_{\mathrm{R}}^\dagger F_{\mathrm{R}} = F_{\mathrm{R}}F_{\mathrm{R}}^\dagger = 1$, N_{R} the particle number operator associated to the right movers, $(a_n, a_n^\dagger)_{n>0}$ a set of bosonic modes indexed by n, and α a regularization parameter that we will identify with the lattice spacing a. The expression of the bosonic field associated to the left movers can be readily deduced from Eq. (5). $F_{\mathrm{L}} = -F_{\mathrm{R}}$, $\phi_{\mathrm{L}}(x) = \phi_{\mathrm{R}}(-x)$. The conjugated fields ϕ, θ are customarily defined as

$$\begin{aligned}\phi(x) &\equiv \frac{-\phi_R(x) + \phi_L(x)}{2} \\ &= -\frac{\pi x}{L}N_R - i\sum_{n>0}\frac{1}{\sqrt{n}}(a_n - a_n^\dagger)\sin\left(\frac{n\pi x}{L}\right)e^{-\alpha\frac{\pi n}{2L}},\end{aligned} \tag{8}$$

$$\begin{aligned}\theta(x) &\equiv \frac{\phi_R(x) + \phi_L(x)}{2} \\ &= \sum_{n>0}\frac{1}{\sqrt{n}}(a_n + a_n^\dagger)\cos\left(\frac{n\pi x}{L}\right)e^{-\alpha\frac{\pi n}{2L}}.\end{aligned} \tag{9}$$

The particle density operator ρ, which counts the number of particle above the Fermi sea, is deduced from $\phi(x)$ through the relation

$$\rho(x) = -\frac{1}{\pi}\partial_x\phi(x). \tag{10}$$

In the remaining, as we want to characterize the zero-energy modes, we will work at half filling. It is important to notice that the definition of the half filling depends on the total number of sites. Let $N_F \in \mathbb{N}$ label the last occupied state of the Fermi sea. For N even, we have $N_F \equiv \frac{N}{2}$. The corresponding momentum is $k_F = \frac{\pi N/2}{a(N+1)} \approx \frac{\pi}{2a} - \frac{\pi}{2aN} \approx \frac{\pi}{2a} - \frac{\pi}{2L}$ to first order in $1/L$. For N odd, the two possible definitions of the half-filled state are $N_F = \frac{N\pm1}{2}$ with corresponding Fermi momenta $k_F = \frac{\pi}{2a} - \frac{\pi}{2L}(1 \mp 1)$. In the remainder of this Letter, we will choose the convention $N_F = \frac{N-1}{2}$ for odd number of sites. The Fermi sea state with all modes filled up to N_F and empty above will be referred to as the *vacuum* state.

Equipped with these relations, we can express the lattice fermionic operator as

$$c_j = \frac{1}{\sqrt{2\pi}}F_{\mathrm{R}}(e^{ik_F x + i\phi_{\mathrm{R}}(x)} - e^{-ik_F x + i\phi_{\mathrm{R}}(-x)}). \tag{11}$$

To derive the Hamiltonian in its bosonized form, we insert expression Eq. (11) into Eq. (1) and discard terms $\propto(-1)^{x/a}$ that are varying fast at the level of the lattice spacing. Because the SSH Hamiltonian itself contains such a fast varying prefactor for the staggering term, this gives contributions $\propto \mathrm{R}^\dagger\mathrm{L}, \mathrm{L}^\dagger\mathrm{R}$ in addition to the usual contribution of the tight-binding term $\propto \mathrm{R}^\dagger\mathrm{R}, \mathrm{L}^\dagger\mathrm{L}$. The result is [see the Supplemental Material (SM) [35] for details]

$$\begin{aligned}H = &\int_0^L dx\frac{v_F}{2\pi}[:(\partial_x\phi)^2: + :(\partial_x\theta)^2:] \\ &+ \frac{\delta}{L\sin\frac{\pi x}{L}}:\cos\left[2\phi(x) + \left(\frac{\pi}{a} - 2k_F - \frac{\pi}{L}\right)x\right]:,\end{aligned} \tag{12}$$

where $v_F := 2ta\sin(k_F a)$ denotes the Fermi velocity and $:\bullet:$ normal ordering of the fermionic modes with respect to the vacuum. To get the normal-ordered expression of the cos term, we used $e^{i\zeta\phi(x)} =: e^{i\zeta\phi(x)}: [\frac{2L}{\pi a}\sin(\frac{\pi x}{L})]^{-\frac{\zeta^2}{4}}$ which itself comes from (8).

We see that the SSH in the bosonized language is almost equivalent to a sine-Gordon Hamiltonian except that the prefactor in front of the sinus has spatial dependence (we mention that the same dependence appeared already in Ref. [21], where a more general noninteracting model is studied).

We now turn to the computation of ρ using the classical Euler-Lagrange (EL) equations of motion. Let $Z \equiv \mathrm{tr}(e^{-\beta H})$ and Π the conjugated field to ϕ, $\Pi \equiv \frac{1}{\pi}\partial_x\theta$. In the imaginary-time formalism, we have

$$Z = \int \mathcal{D}\phi\mathcal{D}\Pi e^{\int_0^\beta\int_0^L d\tau dx\mathcal{L}}, \tag{13}$$

with $\mathcal{L}$ the Lagrangian density $\int dx\mathcal{L} = \int dx i\Pi\partial_\tau\phi - H$.

The EL equations $\frac{\partial \mathcal{L}}{\partial \phi} = \frac{\partial}{\partial \tau}\frac{\partial \mathcal{L}}{\partial \partial_\tau \phi} + \frac{\partial}{\partial x}\frac{\partial \mathcal{L}}{\partial \partial_x \phi}$ yield

$$\frac{1}{v_F}\partial_\tau^2\phi + v_F\partial_x^2\phi = -\frac{2\pi\delta}{L\sin\frac{\pi x}{L}}\sin\left[2\phi(x) + \left(\frac{\pi}{a} - 2k_F - \frac{\pi}{L}\right)x\right]. \quad (14)$$

In the zero-temperature limit, all the weight of the probability measure will be contained in the stationary solution $\partial_\tau\phi = 0$. Introducing the natural rescaling $y \equiv x/L$, $\varphi(y) \equiv \phi(yL)$, we get the L-independent equation

$$\partial_y^2\varphi(y) = -\nu\frac{\sin(2\varphi(y) + \epsilon\pi y)}{\sin(\pi y)}, \quad (15)$$

where we introduced $\nu = \frac{2\pi\delta L}{v_F} \approx \frac{\pi\delta(N+1)}{t}$ and $\epsilon = 0$ for an *even* number of sites where $k_F = \frac{\pi}{2a} - \frac{\pi}{2L}$, and $\epsilon = 1$ for an *odd* number of sites using the convention $k_F = \frac{\pi}{2a} - \frac{\pi}{L}$. The boundary conditions for φ are read from Eq. (8): At $y = 0$ we have $\varphi = 0$ and at $y = 1$ we have $\varphi = -\pi n_R$ with n_R the number of particles created on top of the vacuum.

To the best of our knowledge, Eq. (15) has no known analytical solution so we resort to numerics. To assert the validity of our approach, we compare numerical solutions of Eq. (15) with exact diagonalization (ED) results performed on the discrete Hamiltonian Eq. (1) in the zero-temperature ground state. The ED results show fast oscillations on the scale of the lattice spacing $\propto 1/k_F$ that we do not see from the solutions of the EL equations of motion since we precisely discarded these terms. Coarse graining over the fast oscillations gives a smoothly varying density profile on the scale of the total system size. We observe excellent agreement between the ED and the EL solutions—see Fig. 1. We also checked that the agreement holds both for δ positive or negative, for an even or an odd number of sites, and for different values of n_R (corresponding to different excited states) [35].

For the even case and $n_R = 0$ the solution of the EL equations is simply $\phi = 0$ so that $\rho(x) = 0$, which is consistent with the particle-hole symmetry of the model. For $\delta > 0$, fixing $n_R = 1$ amounts to populating the first mode above the vacuum state, i.e., the zero-energy edge mode. From Eq. (10) and Eq. (15), we can thus deduce the density profile of this edge mode. We plot in Fig. 1 the numerical solution of (15) and indeed see a concentration of the density at the boundaries. There is a nice interpretation from Eq. (12). The term proportional to δ wants to lock the field in the minima of the cos term. For N even and $\delta > 0$, this corresponds to $\phi = -\frac{\pi}{2}[\pi]$. To match the boundary condition, the field ϕ must jump from 0 to $-\pi/2$ and then from $-\pi/2$ to $-\pi$. These jumps translate in concentration on the edges for the density $\rho(x) = -\frac{1}{\pi}\partial_x\phi(x)$. The stiffness of the jumps of ϕ is controlled by ν and determines how much the mode is concentrated at the edges. Equation (15) is consistent with the exponential localization of the edge mode near the boundary. Indeed, for small y, one crude approximation of Eq. (15) at first order in y is given by $\partial_y(\partial_y\varphi) \approx -\frac{2\nu}{\pi}\partial_y\varphi$. Using additionally that the total particle number is 1, i.e., $\frac{1}{\pi}\int_0^1 dy\partial_y\varphi(y) = 1$, leads to the following ansatz φ_A when $\nu \gg 1$:

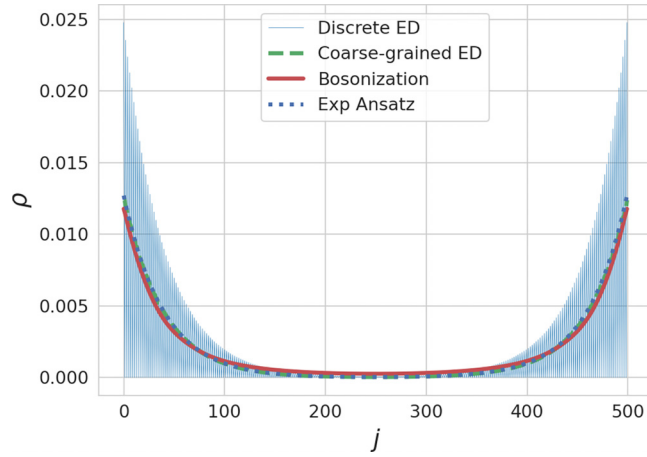

FIG. 1. Comparison between the results of the discrete ED, the bosonization result, and the exponential fit for $\nu = 20$, $N = 500$. The uniform vacuum density $\rho_j = 1/2$ has been subtracted. The light-blue curve corresponds to exact discrete ED result which show fast oscillations at the scale of the lattice spacing. The green dashed curve represents the same data coarse-grained over two sites. The red curve is the density profile obtained by solving the EL equation (15) from the bosonized theory and using $\rho_j = \frac{1}{2} - \frac{1}{\pi}\partial_x\phi(x = ja)$ and $\phi(x = ja) = \phi'(y)$. Lastly, the dashed blue line is obtained from the exponential ansatz Eq. (16). Note that the latter two appear superposed on this plot.

$$\partial_y\varphi_A(y) = -\nu\frac{\cosh\left[\frac{\nu}{\pi}(2y-1)\right]}{\sinh\left(\frac{\nu}{\pi}\right)}. \quad (16)$$

This exponential ansatz dictates the expression for the typical localization length of the edge mode,

$$\ell \equiv \frac{\pi L}{2\nu} = \frac{v_F}{4\delta}. \quad (17)$$

For the free SSH, it is known (see, e.g., Refs. [29,30]) that $\ell \propto \frac{a}{\ln\frac{t+\delta}{t-\delta}} \approx \frac{at}{2\delta}$. For $\frac{\delta}{t} \ll 1$, this is consistent with our result since $v_F \approx 2ta$ at half filling. The fact that the result agrees in the limit where $\ell \gg a$ is a consequence of the bosonization procedure, which is a long-wavelength, low-energy theory.

We now turn to interactions. We consider a nearest-neighbor interacting term of the form

$$H_I := V\sum_{j=1}^{N-1}(n_j - 1/2)(n_{j+1} - 1/2), \quad (18)$$

with $n_j := c_j^\dagger c_j$ the particle number operator. Note that this term preserves time-reversal, particle-hole, and chiral symmetries. From now on, we will work exclusively in the topological phase, i.e., $\delta > 0$, N even, and $N_F = \frac{N}{2}$. As usual in bosonization, the effects of interactions are to rescale the coefficients appearing in the free part. Introducing $uK \equiv v_F$

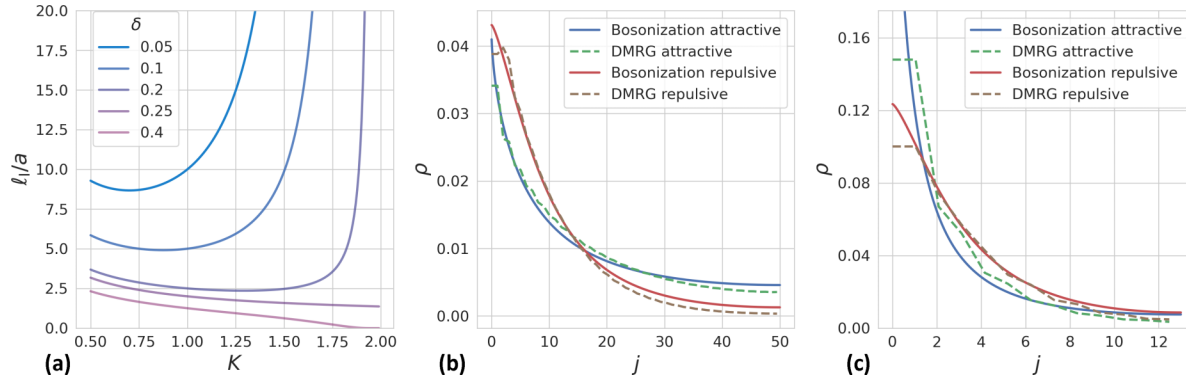

FIG. 2. (a) Plots of relation (23) for the localization length in the interacting case as a function of K for different values of δ. We see that the effect of interactions on the edge mode strongly depends on the value of δ. (b) Comparison between the solution of the EL equations of motion (20) in the interacting case with DMRG simulations. The DMRG results for attractive (repulsive) interactions have been coarse-grained once (twice) over two sites. Only half of the solution is shown for better readability. We took $N = 100$, $\delta = 0.05$, $V = 1.6$, $K = 0.7$ for the repulsive case and $V = -0.77$, $K = 1.4$ for the attractive case. In this case, attractive (repulsive) interactions delocalize (localize) the edge mode. (c) Same as (b) with parameter values $N = 26$, $\delta = 0.2$, $V = 1.6$, $K = 0.7$ for the repulsive case and $V = -0.77$, $K = 1.4$ for the attractive case. We see that, in comparison to (b), the qualitative effects of the interactions are swapped.

and $\frac{u}{K} \equiv v_F + \frac{4Va}{\pi}$, we obtain [35]

$$H = \int_0^L dx \left[\frac{1}{2\pi} \left(\frac{u}{K} : (\partial_x \phi)^2 :_{\mathrm{I}} + uK : (\partial_x \theta)^2 :_{\mathrm{I}} \right) + \delta \left(\frac{2}{a\pi} \right)^{1-K} \frac{1}{\left(L \sin \frac{\pi x}{L} \right)^K} : \cos(2\phi) :_{\mathrm{I}} \right]. \quad (19)$$

Because the free part of the Hamiltonian has been rescaled by interactions, the normal ordering is now with respect to the new "squeezed" vacuum which we denote by $::_{\mathrm{I}}$. The new normal-ordering relation is obtained by rescaling the fields accordingly to the new vacuum $\phi \to K^{1/2}\phi$, $\theta \to K^{-1/2}\theta$, leading to $e^{i\zeta\phi} =: e^{i\zeta\phi} :_{\mathrm{I}} [\frac{2L}{\pi a} \sin(\frac{\pi x}{L})]^{-\frac{K\zeta^2}{4}}$.

In principle, since we are at half filling, there should also be an umklapp term $\propto \cos(4\phi)$ [35]. For simplification, we will neglect this contribution in the present work by restricting ourselves to the case $K > 1/2$ for which it is irrelevant in the renormalization group (RG) sense. The EL equations of motion in the presence of interactions become

$$\partial_y^2 \varphi(y) = -2 \left(\frac{L}{a} \right)^2 \left(\frac{a\pi}{2L} \right)^K K^2 \frac{\delta}{t} \frac{\sin(2\varphi)}{[\sin(\pi y)]^K}. \quad (20)$$

A comparison of numerical solutions of (20) and density-matrix renormalization group (DMRG) simulations is shown in Fig. 2(b) for $\delta = 0.05$, $N = 100$ and $V = 1.6$, $K = 1.4$ for the attractive case and $V = -0.77$, $K = 1.4$ for the repulsive case. We see that the EL equations of motion predicts the correct density profile. For these parameters, we see that attractive interactions delocalize the edge mode into the bulk while repulsive interactions localize it further.

For $1/2 < K < 2$, we can give an estimation of the localization length by expanding Eq. (20) for $y \ll 1$. This gives

$$\partial_y^2 \varphi(y) = -\left(\frac{2L}{a} \right)^{2-K} K^2 \frac{\delta}{t} \frac{\varphi(y)}{y^K}. \quad (21)$$

Imposing $\varphi(y) = 0$, the solutions to this equation are of the form

$$\phi(x \ll L) = \sqrt{\frac{x}{L}} J_{\frac{1}{|2-K|}} \left[\left(\frac{2x}{a} \right)^{\frac{2-K}{2}} \left(\frac{\delta}{t} \right)^{\frac{1}{2}} \frac{2K}{|2-K|} \right], \quad (22)$$

where J_α is the Bessel function of the first kind—see SM [35] for the proof. The precise shape of the Bessel function depends on α but, as one can easily verify, the position of the first maximum of J_α scales linearly with α. Thus, we define the localization length to be the value ℓ_{I} such that $\varphi(\ell_{\mathrm{I}}) = \frac{2}{|2-K|}$ where the factor 2 has been put in order to match with the localization length of the free case. Following this definition, we obtain that

$$\ell_{\mathrm{I}} = \frac{a}{2} \left(\frac{t}{\delta K^2} \right)^{\frac{1}{2-K}}. \quad (23)$$

The localization length diverges at $K = 2$ if $\frac{\delta}{t} < \frac{1}{4}$. This gives a rough criteria for having a localized mode in the attractive regime $K > 1$. Importantly, note that ℓ_{I} is not, in general, a monotonic function of K [see Fig. 2(a)].

One consequence of this is that attractive or repulsive interactions do not *systematically* delocalize or localize the edge mode, and their effect can change depending on the value of δ. This is illustrated in Fig. 2(c) where we took $\delta = 0.2$. Contrary to the previous case shown in Fig. 2(b), we see that the effects of attractive interactions are to *localize* the edge mode further to the boundary and the other way around for the repulsive ones.

Finally, note that from the standard RG argument [17], the scaling of the gap in the vertical regime of the flow (i.e., K constant and δ small) is given by $\Delta \approx \frac{2t}{K} (\frac{2\delta K}{t})^{\frac{1}{2-K}}$. Thus, in the region $1/2 < K < 2$ the localization length Eq. (23) scales roughly as $1/\Delta$. One interpretation is that Δ represents the cost for the edge mode to "penetrate" the system and, as such, the greater Δ is, the smaller is ℓ_{I}.

Conclusion. In this Letter, we derived the bosonized theory of the interacting SSH model with open boundaries. One of our remarkable results is that attractive (repulsive) interactions

do not systematically delocalize or localize the edge mode, but this behavior is strongly dependent on the value of the staggering parameter δ. Note that while we only considered nearest-neighbor interactions, bosonization naturally allows us to treat long-ranged interactions.

Importantly, our study offers quantitative arguments to determine the effects of interactions on the edge mode and pave the way to study other interacting topological models. Indeed, the main ingredients allowing us to derive the edge mode physics are a free bosonic Hamiltonian, a sine-Gordon-type term, and the correct normal ordering of these terms by taking into account the open boundaries. All these features are also present in other 1D topological models presenting edge modes such as the spin-1 antiferromagnetic Heisenberg chain [36–38], the Affleck-Kennedy-Lieb-Tasaki (AKLT) model [39], or the Kitaev fermionic chain [21,40].

Finally, it is noteworthy that the physics of the edge modes in these models has been recently investigated in quantum simulation platforms [41,42].

The DMRG simulations presented in this Letter were done using the TENPY package for tensor network calculations with PYTHON [43]. T.J. thanks Aashish Clerk for interesting discussions and comments on this work. The authors acknowledge support from the Swiss National Science Foundation under Division II .

[1] F. D. M. Haldane, Nobel lecture: Topological quantum matter, Rev. Mod. Phys. **89**, 040502 (2017).
[2] A. Altland and M. R. Zirnbauer, Nonstandard symmetry classes in mesoscopic normal-superconducting hybrid structures, Phys. Rev. B **55**, 1142 (1997).
[3] C.-K. Chiu, J. C. Y. Teo, A. P. Schnyder, and S. Ryu, Classification of topological quantum matter with symmetries, Rev. Mod. Phys. **88**, 035005 (2016).
[4] M. Nakahara, *Geometry, Topology and Physics* (CRC Press, Boca Raton, FL, 2018).
[5] J. Cayssol and J. N. Fuchs, Topological and geometrical aspects of band theory, J. Phys. Mater. **4**, 034007 (2021).
[6] K. v. Klitzing, G. Dorda, and M. Pepper, New Method for High-Accuracy Determination of the Fine-Structure Constant Based on Quantized Hall Resistance, Phys. Rev. Lett. **45**, 494 (1980).
[7] K. von Klitzing, T. Chakraborty, P. Kim, V. Madhavan, X. Dai, J. McIver, Y. Tokura, L. Savary, D. Smirnova, A. M. Rey, C. Felser, J. Gooth, and X. Qi, 40 years of the quantum Hall effect, Nat. Rev. Phys. **2**, 397 (2020).
[8] L. Fu and C. L. Kane, Superconducting Proximity Effect and Majorana Fermions at the Surface of a Topological Insulator, Phys. Rev. Lett. **100**, 096407 (2008).
[9] C. L. Kane and E. J. Mele, Quantum Spin Hall Effect in Graphene, Phys. Rev. Lett. **95**, 226801 (2005).
[10] B. A. Bernevig, T. L. Hughes, and S.-C. Zhang, Quantum spin Hall effect and topological phase transition in HgTe quantum wells, Science **314**, 1757 (2006).
[11] C. Nayak, S. H. Simon, A. Stern, M. Freedman, and S. Das Sarma, Non-Abelian anyons and topological quantum computation, Rev. Mod. Phys. **80**, 1083 (2008).
[12] R. B. Laughlin, Anomalous Quantum Hall Effect: An Incompressible Quantum Fluid with Fractionally Charged Excitations, Phys. Rev. Lett. **50**, 1395 (1983).
[13] W. P. Su, J. R. Schrieffer, and A. J. Heeger, Solitons in Polyacetylene, Phys. Rev. Lett. **42**, 1698 (1979).
[14] M. Atala, M. Aidelsburger, J. T. Barreiro, D. Abanin, T. Kitagawa, E. Demler, and I. Bloch, Direct measurement of the Zak phase in topological Bloch bands, Nat. Phys. **9**, 795 (2013).
[15] S. de Léséleuc, V. Lienhard, P. Scholl, D. Barredo, S. Weber, N. Lang, H. P. Büchler, T. Lahaye, and A. Browaeys, Observation of a symmetry-protected topological phase of interacting bosons with Rydberg atoms, Science **365**, 775 (2019).
[16] F. D. M. Haldane, 'Luttinger liquid theory' of one-dimensional quantum fluids. I. Properties of the Luttinger model and their extension to the general 1D interacting spinless Fermi gas, J. Phys. C **14**, 2585 (1981).
[17] T. Giamarchi, *Quantum Physics in One Dimension* (Oxford University Press, Oxford, U.K., 2003).
[18] I. Affleck and D. Giuliano, Topological superconductor—Luttinger liquid junctions, J. Stat. Mech. (2013) P06011.
[19] S. Gangadharaiah, B. Braunecker, P. Simon, and D. Loss, Majorana Edge States in Interacting One-Dimensional Systems, Phys. Rev. Lett. **107**, 036801 (2011).
[20] A. M. Lobos, R. M. Lutchyn, and S. Das Sarma, Interplay of Disorder and Interaction in Majorana Quantum Wires, Phys. Rev. Lett. **109**, 146403 (2012).
[21] V. Chua, K. Laubscher, J. Klinovaja, and D. Loss, Majorana zero modes and their bosonization, Phys. Rev. B **102**, 155416 (2020).
[22] R.-B. Wang, A. Furusaki, and O. A. Starykh, Majorana end states in an interacting quantum wire, Phys. Rev. B **102**, 165147 (2020).
[23] A. M. Marques and R. G. Dias, Multihole edge states in Su-Schrieffer-Heeger chains with interactions, Phys. Rev. B **95**, 115443 (2017).
[24] D.-B. Zhang, Z. Zheng, Y. X. Zhao, Q.-H. Wang, and Z. D. Wang, Locking of symmetry breaking and topological phase in an interacting fermionic wire, Phys. Rev. Res. **2**, 013122 (2020).
[25] M. Yahyavi, L. Saleem, and B. Hetényi, Variational study of the interacting, spinless Su-Schrieffer-Heeger model, J. Phys.: Condens. Matter **30**, 445602 (2018).
[26] A. A. Nersesyan, Phase diagram of an interacting staggered Su-Schrieffer-Heeger two-chain ladder close to a quantum critical point, Phys. Rev. B **102**, 045108 (2020).
[27] Y.-T. Lin, D. M. Kennes, M. Pletyukhov, C. S. Weber, H. Schoeller, and V. Meden, Interacting Rice-Mele model: Bulk and boundaries, Phys. Rev. B **102**, 085122 (2020).
[28] For a finite system, the two modes are not, strictly speaking, degenerate but their energy approaches zero exponentially fast as one increases the system size.
[29] A. Palyi, J. K. Asboth, and L. Oroszlany, *A Short Course on Topological Insulators*, 1st ed., Lecture Notes in Physics (Springer, Cham, 2016).
[30] J. Dalibard, Cours au Collège de France 2018: La matière topologique et son exploration avec les gaz quantiques, Doctorat, France, 2018 (hal-03746131).

[31] J. von Delft and H. Schoeller, Bosonization for beginners—refermionization for experts, Ann. Phys. **510**, 225 (1998).

[32] M. Fabrizio and A. O. Gogolin, Interacting one-dimensional electron gas with open boundaries, Phys. Rev. B **51**, 17827 (1995).

[33] A. E. Mattsson, S. Eggert, and H. Johannesson, Properties of a Luttinger liquid with boundaries at finite temperature and size, Phys. Rev. B **56**, 15615 (1997).

[34] M. A. Cazalilla, Low-energy properties of a one-dimensional system of interacting bosons with boundaries, Europhys. Lett. **59**, 793 (2002).

[35] See Supplemental Material at http://link.aps.org/supplemental/10.1103/PhysRevB.107.L201111 for contains detailed computation of the main equations presented in the Letter as well as additional plots for different regimes.

[36] F. D. M. Haldane, Nonlinear Field Theory of Large-Spin Heisenberg Antiferromagnets: Semiclassically Quantized Solitons of the One-Dimensional Easy-Axis Néel State, Phys. Rev. Lett. **50**, 1153 (1983).

[37] F. Haldane, Continuum dynamics of the 1-D Heisenberg antiferromagnet: Identification with the O(3) nonlinear sigma model, Phys. Lett. A **93**, 464 (1983).

[38] H. J. Schulz, Phase diagrams and correlation exponents for quantum spin chains of arbitrary spin quantum number, Phys. Rev. B **34**, 6372 (1986).

[39] I. Affleck, T. Kennedy, E. H. Lieb, and H. Tasaki, Rigorous Results on Valence-Bond Ground States in Antiferromagnets, Phys. Rev. Lett. **59**, 799 (1987).

[40] A. Y. Kitaev, Unpaired Majorana fermions in quantum wires, Phys. Usp. **44**, 131 (2001).

[41] P. Sompet, S. Hirthe, D. Bourgund, T. Chalopin, J. Bibo, J. Koepsell, Petar Bojović, R. Verresen, F. Pollmann, G. Salomon *et al.*, Realizing the symmetry-protected Haldane phase in Fermi–Hubbard ladders, Nature (London) **606**, 484 (2022).

[42] X. Mi, M. Sonner, M. Y. Niu, K. W. Lee, B. Foxen, R. Acharya, I. Aleiner, T. I. Andersen, F. Arute, K. Arya, A. Asfaw, J. Atalaya, J. C. Bardin, J. Basso, A. Bengtsson, G. Bortoli, A. Bourassa, L. Brill, M. Broughton, B. B. Buckley *et al.*, Noise-resilient edge modes on a chain of superconducting qubits, Science **378**, 785 (2022).

[43] J. Hauschild and F. Pollmann, Efficient numerical simulations with Tensor Networks: Tensor Network Python (TeNPy), SciPost Phys. Lect. Notes (2018).